Supplement of Atmos. Meas. Tech., 10, 5063–5073, 2017
https://doi.org/10.5194/amt-10-5063-2017-supplement

Atmospheric Measurement Techniques
Open Access

Supplement of

Improved methods for signal processing in measurements of mercury by Tekran® 2537A and 2537B instruments

Jesse L. Ambrose

Correspondence to: Jesse L. Ambrose (Jesse.Ambrose@unh.edu)

S1 Details on the Format of the Tekran® Analyzer's Serial Data Output

The serial data output ("RAWDUMP" format) from the Tekran® analyzer can be parsed into the components listed below. (A more detailed description is provided in the Tekran® user manuals [*c.f.*, Tekran Corporation, 2006, 2007].)

I. A "Raw data" string, which consists of Hg atomic fluorescence signal values, recorded at 10 Hz over a user-defined interval of the sample analysis cycle.

II. A "Peak table" string, which consists of a header and parameters defining the Hg thermal desorption peak profile (*e.g.*, the peak start and end times) according to the Tekran® analyzer's internal signal processing method.

III. A "Final data" string, which consists of a header and the following components (not ordered exactly as in the string): the timestamp; the cycle type flag ("CLN", clean cycle; "CONT", continuous ambient air analysis cycle; "SPAN", calibration gas analysis cycle; "ZERO", zero air blank cycle); the Au trap identity ("A" or "B"); the sample duration (seconds) and volume (standard liters); the area of the Hg TD peak, as determined by the Tekran® analyzer's internal signal processing method, and the corresponding Hg concentration, calculated based on the sample volume, Hg TD peak area, and internal calibration data (see below); and some diagnostic parameters (*e.g.*, the baseline standard deviation).

An example string for a single sample cycle is shown in Fig. S1. An additional "Calibration data" string is generated when a calibration gas analysis cycle is executed (Fig. S2).

```
RAWDUMP:
 110358 110430 110463 110468 110445 110433 110460 110455 110461 110456
 110458 110414 110416 110429 110421 110428 110459 110471 110481 110508
 110528 110539 110561 110554 110571 110595 110612 110607 110620 110642
 110650 110624 110656 110686 110725 110770 110799 110863 110926 110973
 111056 111131 111206 111318 111415 111570 111732 111880 112027 112198
 112389 112598 112830 113105 113393 113763 114164 114634 115106 115634
 116179 116842 117517 118266 119019 119802 120694 121636 122564 123553
 124546 125510 126511 127496 128405 129364 130184 131003 131714 132390
 132967 133531 133945 134334 134595 134843 135010 135123 135235 135235
 135204 135115 135061 134908 134723 134538 134285 133996 133708 133293
 132900 132480 132024 131531 131054 130494 129982 129432 128870 128318
 127814 127241 126708 126158 125618 125094 124615 124162 123714 123240
 122802 122409 122006 121592 121194 120860 120489 120145 119810 119469
 119146 118803 118516 118203 117911 117611 117379 117082 116826 116607
 116369 116205 115967 115769 115590 115396 115258 115034 114857 114683
 114530 114292 114118 113944 113782 113633 113493 113314 113176 113066
 112932 112814 112702 112583 112517 112374 112285 112205 112086 111974
 111876 111770 111698 111562 111450 111345 111274 111177 111087 111036
 110969 110944 110922 110863 110824 110764 110711 110631 110570 110513
 110492 110392 110307 110221 110169 110121 110059 109991 109970 109912
 109901 109875 109843 109815 109794 109730 109697 109696 109675 109643
 109582 109515 109494 109465 109412 109395 109349 109341 109291 109260
 109211 109228 109200 109218 109202 109181 109165 109120 109093 109069
 109088 109050 109001 108971 108939 108928 108944 108902 108883 108841
 108848 108886 108861 108894 108894 108852 108844 108807 108799 108788
 108769 108714 108708 108665 108650 108625 108626 108621 108594 108571
 108547 108580 108542 108534 108530 108481 108457 108447 108468 108444
 108437 108393 108387 108399 108396 108362 108311 108289 108265 108243
 108223 108267 108260 108251 108251 108250 108257 108204 108205 108169
 108192 108165 108135 108085 108115 108071 108076 108067 108025 108026
 108008 108034 108011 107983 108011 108028 108037 108033 108009 108027
 108045 108012 107995 107966 107912 107875 107890 107914 107914 107918
 107897 107895 107861 107871 107883 107849 107836 107844 107848 107803
 107784 107730 107729 107688 107708 107711 107744 107731 107706 107719
 107718 107726 107709 107657 107638 107703 107701 107710 107719 107737
 107737 107717 107683 107628 107609 107532 107524 107505 107498 107520
 107513 107569 107531 107546 107550 107553 107525 107521 107533 107510
 107522 107502 107495 107473 107470 107467 107441 107443 107437 107412
 107426 107462 107474 107457 107463 107456 107449 107456 107472
 -9999
-
PEAK    SBL STM   PKHT MXTM    EBL  ETM WIDTH    AREA
PK01 110443  16 135235  90 108866 240  22.4   763347
RAW END:
-
 Date    Time  Typ  C Stat  AdTim    Vol   Bl  BlDev  MaxV    Area    ng/m3
13-12-20 19:19:05 CLN  A OK  0    0    .00 0.553  0.232 0.676  763347    0.000
```

"Raw data" string

"Peak table" string

"Final data" string

Figure S1: An example of the Tekran® 2537B instrument's serial data output ("RAWDUMP" format). The string of 10 Hz Hg fluorescence signal values in the "Raw data" string is delimited at the beginning and end by lines reading "RAWDUMP:" and "-9999", respectively. The data values in the "Peak table" string are delimited at the beginning by a line reading "-" and at the end by a line reading "RAW END:" in the "Final data" string. The "Final data" string is delimited at the beginning by the line reading "RAW END:" and at the end by the line reading "RAWDUMP:" from the subsequent sample's "Raw data" string. Note that the lines containing the dash, "-", and the data header in the "Final data" string are only written with the raw data for the first sample analyzed. The same formatting is used with the 2537A instrument. Further information is provided in the Tekran® user manuals (Tekran Corporation, 2006, 2007).

```
-
CALIBRATION:  S/N:0336   H/W: 3.20   S/W: 1.11     13-12-21   01:33:09
-
ZERO:  A
Sample :   150 sec  |  BlArea :     0
Volume :  2.49 l    |  BlCorr :     0/l
Baseline: 0.498 V    |  PkMax   :  .000 V
Bl StDev:  0.34 mv   |  PkWid   :    .0 sec
Start   : 13-12-21     01:23:11
-
ZERO:  B
Sample :   150 sec  |  BlArea :     0
Volume :  2.50 l    |  BlCorr :     0/l
Baseline: 0.497 V    |  PkMax   :  .000 V
Bl StDev:  0.38 mv   |  PkWid   :    .0 sec
Start   : 13-12-21     01:25:41
-
SPAN:  A    SOURCE
Sample :   150 sec  |  Area    :5796730
Volume :  2.50 l    |  AdjArea :5796730 *
HgAmt   :  105.0pg   |  RespFctr:55191e3
Baseline: 0.496 V    |  PkMax   : 1.873 V
Bl StDev:  0.47 mv   |  PkWid   :  24.2 sec
Start   : 13-12-21     01:28:11
-
SPAN:  B    SOURCE
Sample :   150 sec  |  Area    :5354910
Volume :  2.50 l    |  AdjArea :5354910 *
HgAmt   :  105.0pg   |  RespFctr:50985e3
Baseline: 0.496 V    |  PkMax   : 1.842 V
Bl StDev:  0.33 mv   |  PkWid   :  24.1 sec
Start   : 13-12-21     01:30:41
-
```

Figure S2: An example of the "Calibration data" string in the Tekran® analyzer's serial data output ("RAWDUMP" format). Further information is provided in the Tekran® user manuals (Tekran Corporation, 2006, 2007).

S2 Details on Tekran® Operating Parameters Employed in This Work

Instrument operating parameters and Hg thermal desorption peak integration parameters employed with the Tekran® 2537A and 2537B instruments I tested are given in Table S1.

Table S1. Operating parameters and Hg TD peak integration parameters employed with the Tekran® 2537A and 2537B instruments I tested.[a]

Flow Parameters (mL/min)					
	Car-Meas	Car-Idle	Car-Flush	Smpl-Rate[b]	
	80.0	15.0	160.0	1.00	
Analysis Timing Parameters (sec)					
Sample	Flush-Hi	Meas-dly	BL-time	Intg-dly	Pk-time
150.0	30.0	5.0	10.0	10.0	19.0
Integration Parameters[c]					
N-up	V-up (LSB)	N-dn	V-dn (LSB)	N-base	V-base (LSB)
7	4	3	3	5	8

[a]Parameters are defined in the Tekran® instrument manuals (Tekran Corporation, 2006, 2007). Flows are referenced to standard temperature and pressure of 273.15 K and 1.01325 bar.
[b]Units are liters/min.
[c]LSB: least significant bit (1 LSB ≈ 5 µV).

S3 Details on Constraining the Hg Thermal Desorption Peak End Time

For the dataset represented in Fig. 2 in the main manuscript, the SPAN samples (Hg loadings ≈ 150 pg) have peak heights that are large enough that it is necessary to constrain t_{end} so that it is no later than 10 ds before the upper bound time, t_n, of the interval during which the Hg atomic fluorescence signal was recorded. Two blank samples have peak heights that are small enough that it is necessary to constrain t_{end} so that it is no earlier than 10 ds after the peak maximum time.

For the dataset represented in Fig. S3, the preliminary peak height value is negative for seven blank samples ($VI_{a,a}$ method only). Only the SPAN samples (Hg loadings ≈ 100 pg) have peak heights that are large enough that it is necessary to constrain t_{end} so that it is no later than 10 ds before the upper bound time, t_n, of the interval during which the Hg AF signal was recorded. Sixteen ($VI_{a,a}$ method) and one ($VI_{m,a}$ method) blank samples have peak heights that are small enough that it is necessary to constrain t_{end} so that it is no earlier than 10 ds after the peak maximum time.

S4 Details on Estimating the Baseline Standard Deviation

LabVIEW calculates the mean Bisquare regression residual, r_{mean}, from eq. 1:

$$r_{\text{mean}} = \frac{1}{N} \times \left(\sum_{n=0}^{N-1} w_n \, (f_n - y_n)^2\right) \quad (1)$$

Here, N is the number of data points in the regression, w_n is the weight of the nth data point, f_n is the value of the nth data point predicted by the regression equation, y_n is the true value of the nth data point, and the summation is over all data points. Accordingly, I estimate the baseline standard deviation from r_{mean} using eq. 2:

$$\sigma_{\text{bl}} = \left(r_{\text{mean}} \times \frac{N}{N-1}\right)^{0.5} \quad (2)$$

S5 Results Obtained with a Tekran® 2537B Hg Vapor Analyzer

The test dataset collected with the 2537B instrument is shown as a time series in Fig. S3. Figure S4 shows the Hg thermal desorption profile recorded for a calibration gas analysis cycle. Figure S5 compares Hg loadings derived from the Tekran® method with concentrations derived from the $VI_{m,m}$ method (dataset shown in Fig. S3, excluding SPANs).

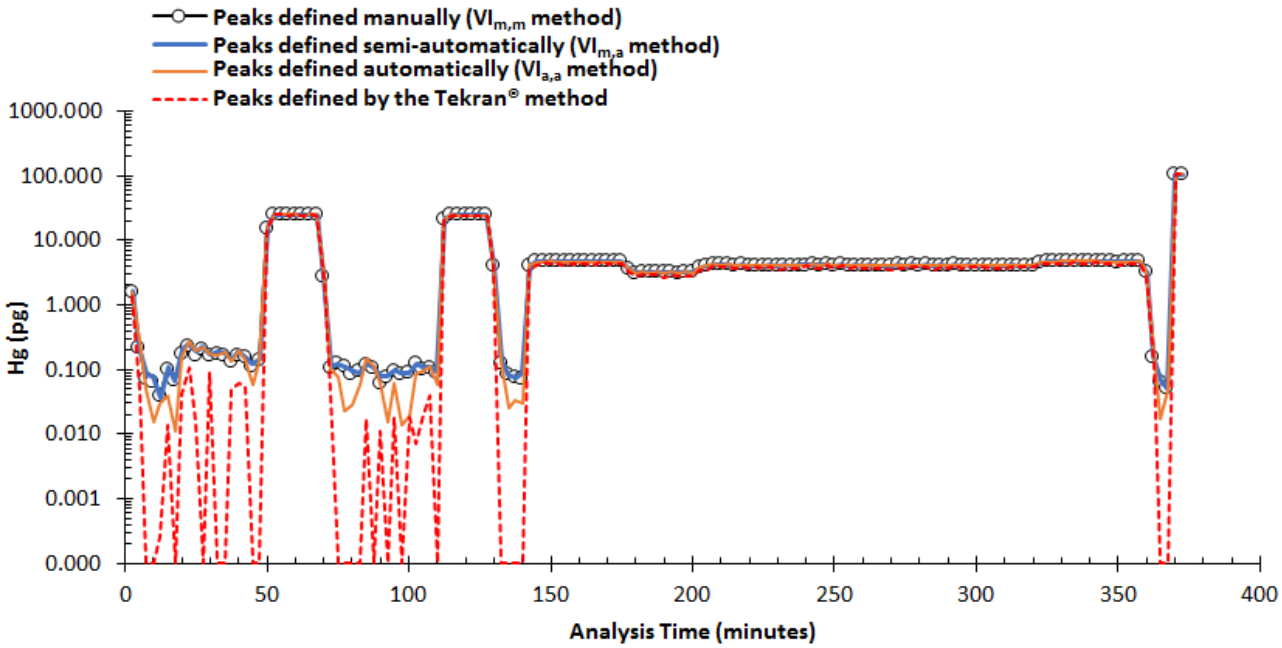

Figure S3: Test dataset collected with a Tekran® 2537B instrument, represented as Hg loadings derived from my VI-based manual, semi-automated, and automated peak height determination methods (the $VI_{m,m}$, $VI_{m,a}$, and $VI_{a,a}$ methods, respectively), and by the Tekran® method. Mercury thermal desorption peaks not detected by the Tekran® method are assigned a value of 0.0001 pg. The pair of data points at ~100 pg corresponds with a pair of calibration gas analysis cycles (SPAN samples), which I use to initialize the VI. I use response factors calculated from the SPAN samples (and the preceding pair of blanks) to calculate Hg loadings for all other samples in the dataset. The sets of data points at ~20 pg correspond with calibration gas analysis cycles using an external calibration unit (external SPAN samples). The external calibration unit is described in Ambrose et al. (2015). The mean value of the baseline standard deviation, σ_{bl} (defined in Sect. 2.1.1 in the main manuscript), is ~0.19 mV (equal to ~0.02 pg). The corresponding estimated lower-limit *f* value (mean ± 2σ) is 1.36(5) × 10^{-4}.

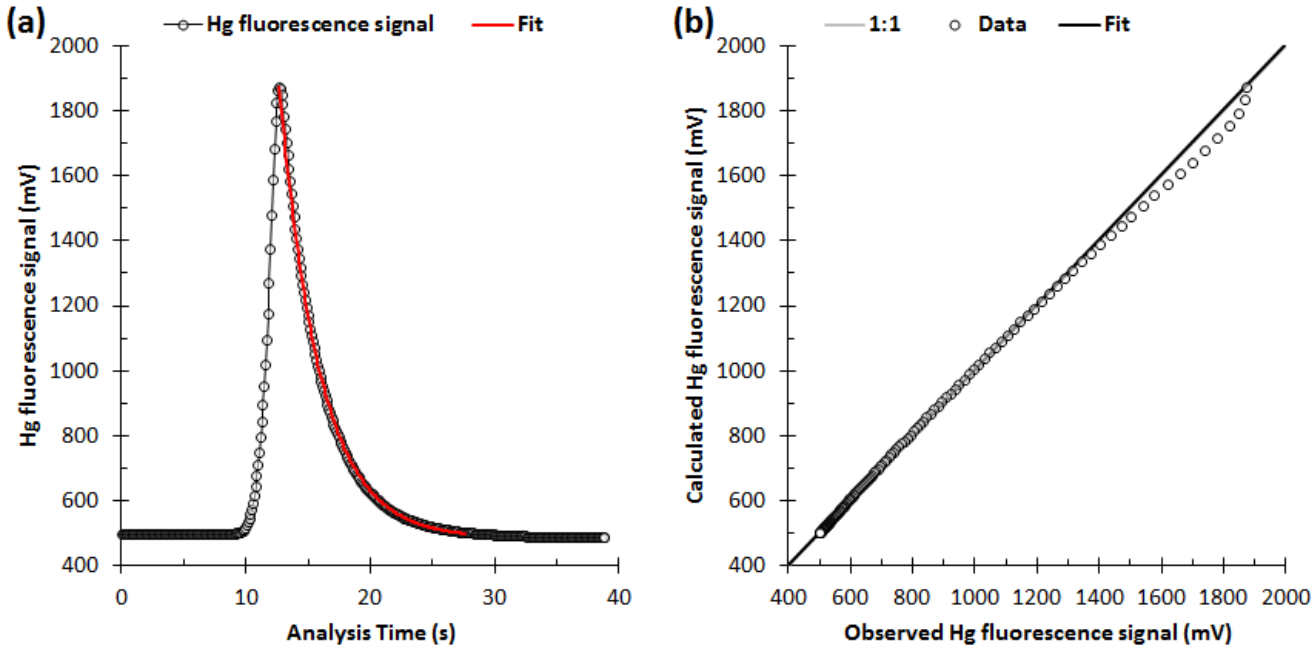

Figure S4: (a) Example Hg thermal desorption profile during a calibration gas analysis cycle on a Tekran® 2537B instrument. Also shown is the corresponding 150 point exponential Bisquare (unweighted) regression (eq. 1 in the main manuscript; r^2 = 0.997) used to derive the decay constant (b = −0.0308 ± 0.0004 ds^{-1}) during initialization of the VI's signal processing method. (b) Comparison between the calculated (fit) and observed Hg atomic fluorescence signal values in (a). The slope and intercept of the linear regression are 1.00 ± 0.01 and 0 ± 7 mV, respectively.

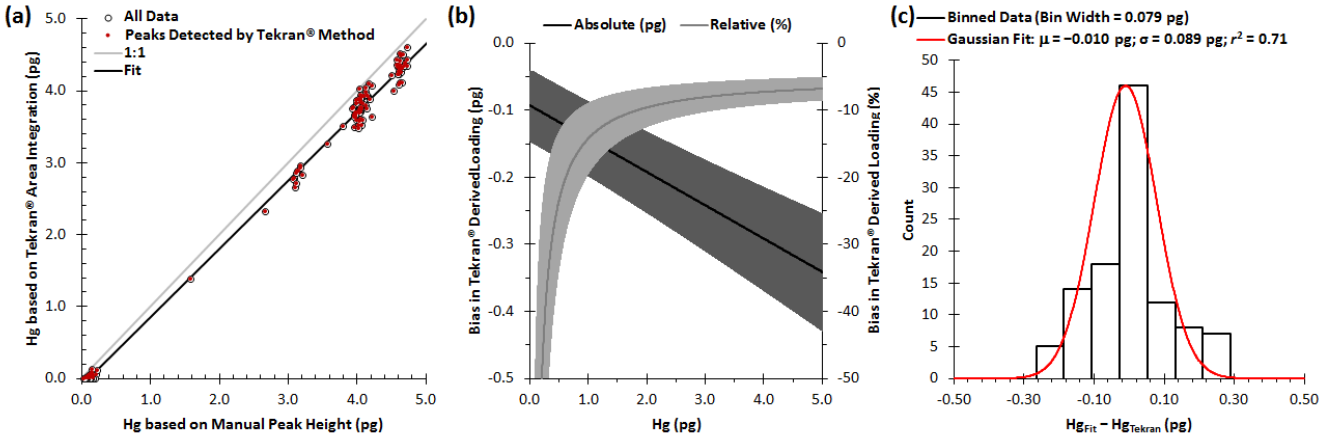

Figure S5: (a) Comparison of Hg loadings derived from measurements made with a Tekran® 2537B instrument using the Tekran® method and my VI-based peak height determination method (dataset shown in Fig. S3, excluding SPANs), with the peaks defined manually (the $VI_{m,m}$ method). The equation of the linear regression is $y = 0.95(1)x - 0.09(5)$ pg ($r^2 = 0.994$, $n = 110$). The fit includes only the data derived from detected peaks (represented by the filled symbols). (b) Absolute and relative biases in the Tekran®-derived loadings, based on the fit in panel (a), where absolute bias ≡ $Hg_{Tekran} - Hg_{Benchmark}$, and relative bias ≡ $100 \times (Hg_{Tekran} - Hg_{Benchmark}) \div Hg_{Benchmark}$. Here "$Hg_{Tekran}$" and "$Hg_{Benchmark}$" represent Hg loadings derived from the Tekran® and $VI_{m,m}$ methods, respectively. Grey bands represents propagated uncertainties (95% confidence intervals) in the fit parameters. (c) Distribution of residuals from panel (a), including only data derived from detected peaks.

The nominal Hg limit of detection for the Tekran® method is 0.5 pg (see Sect. S7). While many Hg thermal desorption peaks in the 2537B dataset are detected by the Tekran® method at Hg loadings <0.5 pg, some Hg TD peaks are undetected by the Tekran® method for loadings ≤0.20 pg (Fig. S3). The results suggest that the actual Hg LOD achieved with the Tekran® method is ~0.2 pg, which is lower than the nominal value (and lower than observed for the 2573A instrument) as a result of modifications that were made to the 2537B instrument to improve its signal-to-noise ratio (Ambrose et al., 2013).

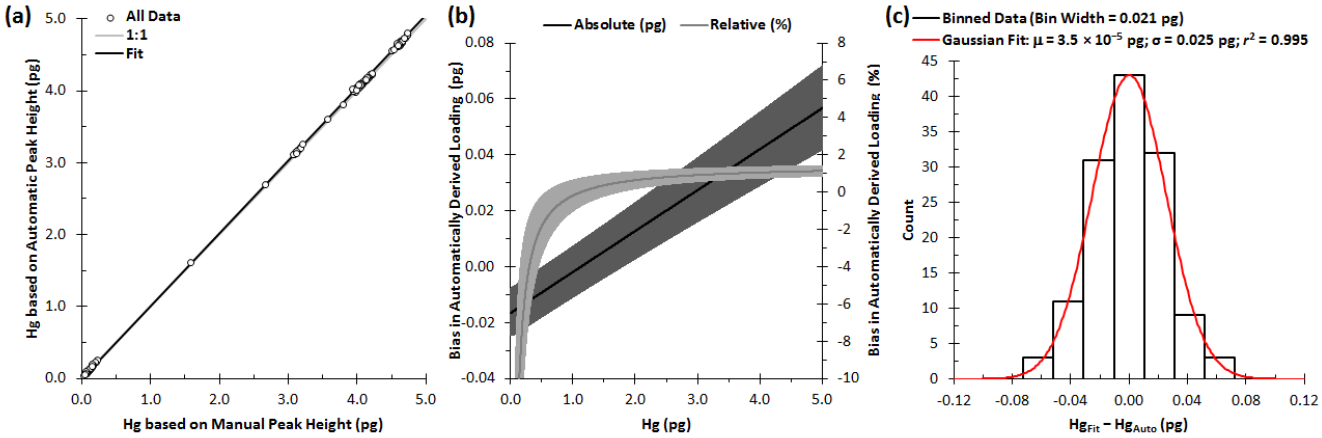

Figure S6: (a) Comparison of Hg loadings derived from measurements made with a Tekran® 2537B instrument using my VI-based automated and manual peak height determination methods (the $VI_{a,a}$ and $VI_{m,m}$ methods, respectively; dataset shown in Fig. S3, excluding SPANs). The equation of the linear regression is $y = 1.015(2)x - 0.017(8)$ pg ($r^2 = 0.9998$, $n = 132$). (b) Absolute and relative biases in the VI-based Hg loadings, based on the fit in panel (a), where absolute bias ≡ $Hg_{Auto} - Hg_{Benchmark}$, and relative bias ≡ 100 × ($Hg_{Auto} - Hg_{Benchmark}$) ÷ $Hg_{Benchmark}$. Here "Hg_{Auto}" and "$Hg_{Benchmark}$" represent Hg loadings derived from the $VI_{a,a}$ and $VI_{m,m}$ methods, respectively. Grey bands represents propagated uncertainties (95% confidence intervals) in the fit parameters. (c) Distribution of residuals from panel (a).

Table S2. Bias in Hg loadings derived by applying automated and semi-automated Hg atomic fluorescence signal processing methods to measurements made with a Tekran® 2537B instrument.

	Hg (pg, ng/m^3)[a,b]						
	5, 1	3.75, 0.75	2.5, 0.5	1.25, 0.25	0.5, 0.1	0.25, 0.05	0.125, 0.025
Method	Bias (%)						
Tekran®[c]	−7 ± 2	−7 ± 2	−9 ± 2	−12 ± 4	−24 ± 10	−42 ± 20	−100[f]
$VI_{a,a}$[d]	1.1 ± 0.3	1.0 ± 0.3	0.8 ± 0.4	0.1 ± 0.7	−2 ± 2	−5 ± 3	−11 ± 6
$VI_{m,a}$[e]	0.7 ± 0.2	0.7 ± 0.2	0.9 ± 0.2	1.2 ± 0.4	2.4 ± 0.9	4 ± 2	8 ± 4

[a]Bias values for the Tekran® and $VI_{a,a}$ methods are calculated from the equations of the linear regressions in Figs. S5a and S6a, respectively. Bias values for the $VI_{m,a}$ method are similarly calculated from the linear regression equation given in Table S6 ("Standard" configuration). All bias values are expressed relative to Hg loadings derived by processing the data using manual peak definition (the $VI_{m,m}$ method).
[b]Hg loadings are also expressed in terms of concentrations under the typical Tekran® operating parameters.
[c]Tekran® operating and peak integration parameters are defined in Table S1.
[d]My VI-based peak height determination method, with peak start and end times determined automatically ($VI_{a,a}$).
[e]My VI-based peak height determination method, with peak start times determined manually and peak end times determined automatically ($VI_{m,a}$).
[f]For Hg < the estimated 0.2 pg Tekran® LOD, the true bias is −100%. For clarity, the true bias is substituted for the calculated value.

S6 Details on Reproducing Hg Thermal Desorption Peak Baselines Calculated by the Tekran® Method

I reproduced the Hg thermal desorption peak areas (and thereby the baselines) calculated by the Tekran® method by doing the following: linearly interpolating between consecutive Hg atomic fluorescence signal values; carrying out a stepwise integration over the interval between the baseline start and end times ("STM" and "ETM" in the "Peak table" string in Fig. S1), with the baseline signal values calculated by linearly interpolating between the baseline start and end values ("SBL" and "EBL" in the "Peak table" string in Fig. S1); summing the resulting integrals and multiplying by a factor of 2.5. I found that the values of "SBL" and "EBL" (Fig. S1) are not the same as the signal values recorded at "STM" and "ETM".

S7 Details on Estimating the Nominal Hg Limit of Detection for the Tekran® Method

The Tekran® manuals (Tekran Corporation, 2006, 2007) state a Hg limit of detection for the Tekran® analyzer of 0.1 ng/m^3 for typical operating conditions, which include a sample flow rate of 1.0 liter/min (at standard temperature and pressure of 273.15 K and 1.01325 bar) and a sample duration of 5 min. These conditions yield a sample volume of 5 standard liters. In terms of Hg loading, the nominal LOD is therefore 0.5 pg.

S8 Details on Sensitivity Tests Carried Out with the $VI_{a,a}$ and $VI_{m,a}$ Methods

Tables S3 and S4 show the results of sensitivity tests carried out with the $VI_{a,a}$ and $VI_{m,a}$ methods, respectively, applied to the 2537A dataset. Following each listed modification to the "Standard" $VI_{a,a}$ configuration, I determine σ_{blank} and the parameters of a linear regression of "Hg_{Auto}" vs. "$Hg_{Benchmark}$" (as in Fig. 5a in the main manuscript). For all sensitivity tests, the fit parameters are indistinguishable (at the 95% confidence interval) from those obtained from the values derived from the "Standard" $VI_{a,a}$ configuration (Fig. 5 in the main manuscript).

Table S3. Results of sensitivity tests carried out with the $VI_{a,a}$ method applied to the 2537A dataset (Fig. 2 in the main manuscript).

$VI_{a,a}$ Configuration	Fit Equation[a]	r^2	Hg LOD[b] (pg)
Standard[c]	$y = 1.001(1)x + 0.000(6)$	0.99992	0.12
$-\delta t_{end}$[d,e,f]	$y = 1.002(2)x - 0.007(7)$	0.99989	0.13
$+\delta t_{end}$[e,g,h]	$y = 1.001(2)x + 0.003(6)$	0.99991	0.11
Δt_{start}[i,j]	$y = 1.000(2)x + 0.001(8)$	0.99988	0.13
$-\delta t_{end}$, Δt_{start}[k]	$y = 1.001(2)x - 0.01(1)$	0.99988	0.17
$+\delta t_{end}$, Δt_{start}[l]	$y = 1.000(2)x + 0.005(8)$	0.99988	0.12
Second SPANs[m]	$y = 1.000(2)x + 0.001(8)$	0.99987	0.13

[a]Units of y are pg. Errors are quoted at the 95% confidence interval (n = 152).
[b]Estimated as twice the standard deviation in blank samples (n = 62).
[c]$VI_{a,a}$ method initialized with the first pair of SPAN samples in Fig. 2 in the main manuscript.
[d]Same as "Standard" but with δt_{end} subtracted from calculated t_{end} values.
[e]The estimated range in δt_{end} is 7–49 ds.
[f]The value of $|\delta t_{end}|$ is > $|t_{end}|$ for five samples. In those cases, t_{end} is forced to 0 ds.
[g]Same as "$-\delta t_{end}$" but with δt_{end} added to calculated t_{end} values.
[h]The value of t_{end} is <10 ds for two samples. In those cases, δt_{end} is set to 49 ds (*i.e.*, the value estimated for a peak height equal to σ_{bl}.)
[i]Same as "Standard", but with t_{start} values taken from the second pair of SPAN samples in Fig. 2.
[j]The values of t_{start} for the first pair of SPAN samples are 123 ds (Au trap A) and 145 ds (Au trap B). For the second pair of SPAN samples, the values are shifted by −9 and −5 ds to 114 ds and 140 ds for Au traps A and B, respectively.
[k]Same as "$-\delta t_{end}$", but with t_{start} values taken from the second pair of SPAN samples in Fig. 2.
[l]Same as "+δtend", but with t_{start} values taken from the second pair of SPAN samples in Fig. 2.
[m]Same as "Standard", but with the $VI_{a,a}$ method initialized with the second pair of SPAN samples in Fig. 2.

Table S4. Results of sensitivity tests carried out with the $VI_{m,a}$ method applied to the 2537A dataset (Fig. 2 in the main manuscript).

$VI_{m,a}$ Configuration	Fit Equation[a]	r^2	Hg LOD[b] (pg)
Standard[c]	$y = 1.001(1)x + 0.004(3)$	0.99998	0.10
$-\delta t_{end}$[d,e]	$y = 1.000(1)x + 0.001(3)$	0.99998	0.10
$+\delta t_{end}$[e,f]	$y = 1.000(1)x + 0.008(3)$	0.99998	0.10
Second SPANs[g]	$y = 1.001(1)x + 0.007(3)$	0.99998	0.10

[a]Units of y are pg. Errors are quoted at the 95% confidence interval (n = 152).
[b]Estimated as twice the standard deviation in blank samples (n = 62).
[c]$VI_{m,a}$ method initialized with the first pair of SPAN samples in Fig. 2 in the main manuscript.
[d]Same as "Standard" but with δt_{end} subtracted from calculated t_{end} values.
[e]The estimated range in δt_{end} is 7–16 ds.
[f]Same as "$-\delta t_{end}$" but with δt_{end} added to calculated t_{end} values.
[g]Same as "Standard", but with the $VI_{m,a}$ method initialized with the second pair of SPAN samples in Fig. 2.

Tables S5 and S6 show the results of sensitivity tests carried out with the $VI_{a,a}$ and $VI_{m,a}$ methods, respectively, applied to the 2537B dataset. Following each listed modification to the "Standard" $VI_{a,a}$ configuration, I determine σ_{blank} and the parameters of a linear regression of "Hg_{Auto}" vs. "$Hg_{Benchmark}$". Because only one pair of SPAN samples was analyzed, the sensitivity of the results to variability in t_{start} can't be tested as is done for the 2537A dataset. However, the values of t_{start} calculated for external standard samples falls within a range of ±5 ds from one another, suggesting that derived Hg loadings would be insensitive to the choice of calibration standard samples used to initialize the VI.

For all sensitivity runs (except the "$+\delta t_{end}$" and "External SPANs" runs) carried out with the $VI_{a,a}$ method (Table S5), and for all sensitivity runs carried out with the $VI_{m,a}$ method (Table S6), the fit parameters are indistinguishable (at the 95% CI) from those obtained from the values derived from the "Standard" $VI_{a,a}$ and $VI_{m,a}$ configurations. For the "$+\delta t_{end}$" sensitivity run carried out with the $VI_{a,a}$ method, bias in "Hg_{Auto}" is slightly lower at high loading and slightly higher at low loading than for the "Standard" VI configuration. For the "External SPANs" run carried out with the $VI_{a,a}$ method, bias in "Hg_{Auto}" is slightly lower than for the "Standard" configuration at all loadings.

Table S5. Results of sensitivity tests carried out with the $VI_{a,a}$ method applied to the 2537B dataset (Fig. S3).

$VI_{a,a}$ Configuration	Fit Equation[a]	r^2	Hg LOD[b] (pg)
Standard[c]	$y = 1.015(2)x - 0.017(8)$	0.9998	0.13
$-\delta t_{end}$[d,e,f]	$y = 1.017(2)x - 0.027(9)$	0.9998	0.13
$+\delta t_{end}$[e,g,h]	$y = 1.007(3)x + 0.016(9)$	0.9998	0.15
External SPANs[i]	$y = 1.008(2)x - 0.002(7)$	0.99988	0.12

[a]Units of y are pg. Errors are quoted at the 95% confidence interval (n = 132).
[b]Estimated as twice the standard deviation in blank samples (n = 37).
[c]$VI_{a,a}$ method initialized with the pair of SPAN samples in Fig. S3.
[d]Same as "Standard" but with δt_{end} subtracted from calculated t_{end} values.
[e]The estimated range in δt_{end} is 2–65 ds.
[f]The value of $|\delta t_{end}|$ is > $|t_{end}|$ for 24 samples. In those cases, t_{end} is forced to 0 ds.
[g]Same as "$-\delta t_{end}$" but with δt_{end} added to calculated t_{end} values.
[h]The value of t_{end} is <10 ds for 16 samples. In those cases, δt_{end} is set to 65 ds (*i.e.*, the value estimated for a peak height equal to σ_{bl}.)
[i]Same as "Standard", but with the $VI_{a,a}$ method initialized with the last pair in the first set of external SPAN samples in Fig. S3.

Table S6. Results of sensitivity tests carried out with the $VI_{m,a}$ method applied to the 2537B dataset (Fig. S3).

$VI_{m,a}$ Configuration	Fit Equation[a]	r^2	Hg LOD[b] (pg)
Standard[c]	$y = 1.005(1)x + 0.009(5)$	0.99994	0.10
$-\delta t_{end}$[d,e,f]	$y = 1.006(1)x + 0.004(5)$	0.99993	0.11
$+\delta t_{end}$[f,g,h]	$y = 1.004(1)x + 0.014(4)$	0.99994	0.10
External SPANs[i]	$y = 1.005(1)x + 0.011(4)$	0.99995	0.10

[a]Units of y are pg. Errors are quoted at the 95% confidence interval (n = 132).
[b]Estimated as twice the standard deviation in blank samples (n = 37).
[c]$VI_{m,a}$ method initialized with the pair of SPAN samples in Fig. S3.
[d]Same as "Standard" but with δt_{end} subtracted from calculated t_{end} values.
[e]The estimated range in δt_{end} is 2–65 ds.
[f]The value of $|\delta t_{end}|$ is > $|t_{end}|$ for four samples. In those cases, t_{end} is forced to 0 ds.
[g]Same as "$-\delta t_{end}$" but with δt_{end} added to calculated t_{end} values.
[h]The value of t_{end} is <10 ds for one sample. In that case, δt_{end} is set to 65 ds (*i.e.*, the value estimated for a peak height equal to σ_{bl}.)
[i]Same as "Standard", but with the $VI_{m,a}$ method initialized with the last pair in the first set of external SPAN samples in Fig. S3.

References

Tekran Corporation: Model 2537A Ambient Mercury Vapour Analyzer User Manual, Rev. 3.01, Tekran Instruments Corporation, Toronto, Canada, 2006.

Tekran Corporation: Model 2537B Ambient Mercury Vapour Analyzer User Manual, Rev. 3.10, Tekran Instruments Corporation, Toronto, Canada, 2007.